

FIG. 2. The three regions of magnetism in the B - A plane [Eqs. (4), (5)]. I, unmagnetized; II, heat magnetism; III, ferromagnetism.

is minimum, which lies roughly midway between T_1 and T_2 of Fig. 1, curve (a), is given by

$$kT_m = \Delta \left[\ln \left(\frac{4B}{1-A} \right) \right]^{-1} \cong B\Delta(1+B)^{-1}. \quad (12)$$

Our model is directly applicable to the thulium intermetallic compounds^{9,8} for which $A < 1$, $B < 1$. However, although the crystal field parameters which determine B/A are not definitely known, it seems most likely that for such systems $(S_b/S_a) < 1$, $B < \frac{1}{4}A$. If $B < \frac{1}{4}A$ then according to (11), $A_m \approx 0.995$ and it is most unlikely that the effect will be found in this class of substances. The effective B/A ratio can be increased, however, by going to a substance wherein the lowest triplet has no matrix ele-

ment of \tilde{S} to the ground singlet. For example, Blume⁵ suggests that in UO_2 the order of levels⁷ is Γ_1 , Γ_5 , Γ_4 , Γ_3 . Letting $A = 2gS_{14}^2/\Delta_{14}$, $B = \frac{1}{2}gS_{55}^2/\Delta_{15}$, in obvious notation, one has⁷ $B/A \approx \frac{1}{4}(\Delta_{14}/\Delta_{15})$, which can be of the order of one. [The expressions derived for the one-triplet model above can be adapted approximately to the two-triplet model if the Boltzmann factor of the upper triplet is neglected. In this case the B^{-1} factor occurring in the exponential factor of Eq. (11) should be replaced by $(3/4B)$.]

*Work supported in part by the National Aeronautics and Space Administration.

†On leave from University of Osaka Prefecture, Osaka, Japan.

¹J. H. Van Vleck, *The Theory of Electric and Magnetic Susceptibilities* (Oxford University Press, New York, 1932), Chap. IX; R. M. Bozorth and J. H. Van Vleck, Phys. Rev. **118**, 1493 (1960).

²R. J. Elliot, in *Magnetism*, edited by G. T. Rado and H. Suhl (Academic Press, Inc., New York, 1965), Vol. IIA, Chap. 7.

³G. T. Trammell, Phys. Rev. **131**, 932 (1963).

⁴B. Bleaney, Proc. Roy. Soc. (London) **A276**, 19 (1963).

⁵M. Blume, Phys. Rev. **141**, 517 (1966).

⁶Y. Ebena and N. Tsuya, Sci. Rep. Res. Inst. Tohoku Univ. Ser. B **12**, Nos. 1, 3, 4 (1960).

⁷K. R. Lea, M. J. M. Leask, and W. P. Wolf, J. Phys. Chem. Solids **23**, 1381 (1962).

⁸Bruce Grover, Phys. Rev. **140**, A1944 (1965).

⁹H. R. Child, M. K. Wilkinson, J. W. Cable, W. C. Koehler, and E. O. Wollan, Phys. Rev. **131**, 922 (1963).

BiSb ALLOY TUNNEL JUNCTIONS

L. Esaki and P. J. Stiles

IBM Watson Research Center, Yorktown Heights, New York

(Received 1 February 1966)

Tunneling spectroscopy has been carried out in the BiSb alloy system to observe changes of the electronic band structure with an increase in Sb concentration. Tunnel junctions were fabricated with a thin insulating layer sandwiched between a single crystal of BiSb alloys, 3.6, 12.0, or 13.5 at.% Sb in Bi, and an evaporated metal layer by a technique previously described.¹ Figures 1(a), 1(b), and 1(c) show plots of conductance of such a sandwich versus voltage at 2°K for 3.6, 12.0, and 13.5% alloys, respectively. The plus voltage indicates a positive-

ly biased evaporated metal electrode in respect to the single-crystal BiSb alloy throughout this report. A W -shape curve in conductance for the 3.6% alloy, reminiscent of the case of pure bismuth,¹ indicates this material to be semimetallic. On the other hand, a large dip² around +10 or +15 mV, seen in Figs. 1(b) and 1(c), shows the existence of the energy gap in these materials. By measurement of the Hall effect, the 12.0 and 13.5% alloys were found to be n -type with 9.3×10^{15} electrons/cm³ and 6.9×10^{15} electrons/cm³, respectively. The voltage at

the bottom of the dip may be equated to

$$10 \text{ or } 15 \text{ meV} = \frac{1}{2}E_G + E_F \sim \frac{1}{2}E_G,$$

where the Fermi energy E_F is about 1 meV or less. Thus, the energy gap E_G is derived

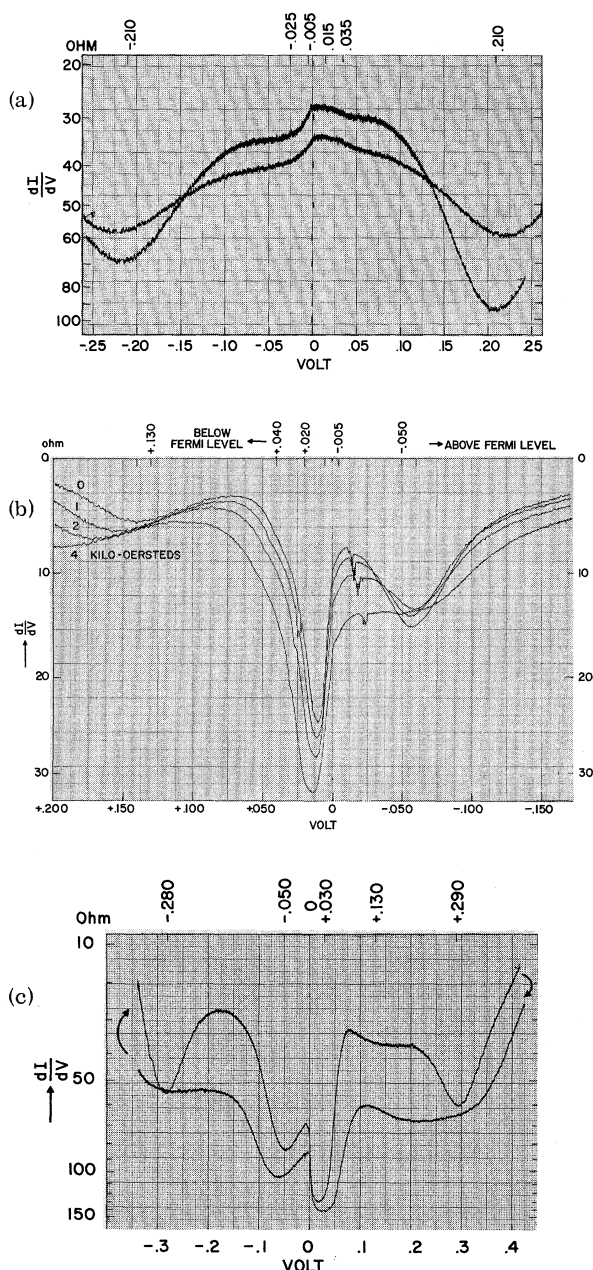


FIG. 1. Conductance versus voltage plots at 2°K. (a) 3.6% alloy tunnel junction; (b) 12.0% alloy tunnel junction, at magnetic fields parallel to the trigonal axis, 0, 1, 2, and 4 kOe; (c) 13.5% alloy tunnel junction, showing a polarization effect, high- and low-conductivity states.

to be 20-30 meV, which is in good agreement with the previous estimate.^{3,4} It is interesting that with an increase in the magnetic field up to 4 kOe, a broad dip around -50 mV tends to be washed away, whereas the dip due to the energy gap is deepened, as seen in Fig. 1(b).

In Figs. 1(b) and 1(c) for semiconducting alloys, one finds major structure corresponding to six band edges: 290, 130, 20-30, ~0, -50, and -280 mV, and minor structure at 40 and -5 mV. These positions were arrived at by treating the conductance as a sum of the conductances from many hole and electron bands, as we did before. Conductance peaks observed in the present experiment, as well as in the previous one,¹ could be attributed to band bending near the surface due to the applied voltage. Figure 2 shows these band edges for semiconducting BiSb alloys together with the case of pure bismuth. Except for the two bands at L_1 , these band edges have not been seen before in the BiSb alloys. A tentative assignment to particular points in the Brillouin zone was made using Mase's calculation,⁵ the argument of Cohen, Falicov, and Golin,⁶ and Hebel and Smith's experiment.⁷ Cohen's notations are used in Fig. 2. According to Mase, the principal change due to the addition of Sb to Bi is a reduction

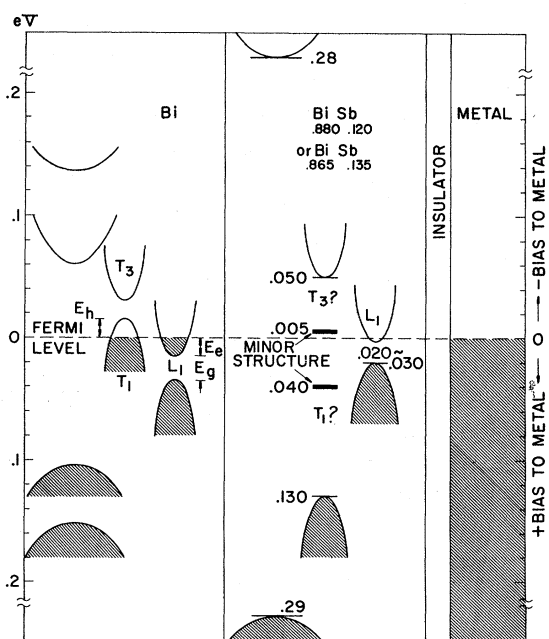


FIG. 2. Band energies for pure Bi and semiconducting BiSb alloys constructed from our tunneling spectroscopy data, and the energy diagram of BiSb-alloy tunnel junction.

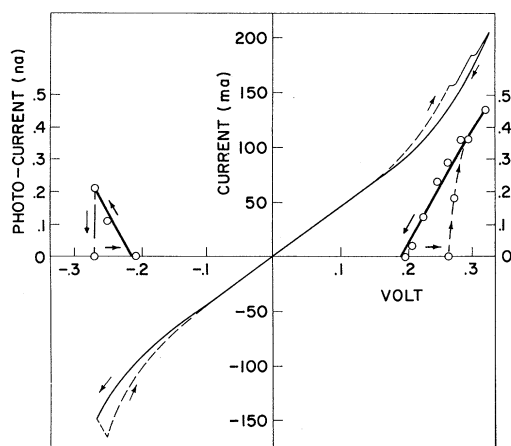


FIG. 3. I - V curve of semiconducting BiSb-alloy tunnel junction in the high-current and -voltage region, and photodetector current corresponding to the applied voltage.

in spin-orbit coupling, which has a small effect on the band edges at L_1 . As shown in the figure, these alloys appear to have become a semiconductor due to widening of the energy gap between T_1 and T_3 , while there is some ambiguity whether the minor structure should be assigned to T_1 and T_3 or not.

We have observed a detectable light emission over the range beyond 100 mA in both directions of semiconducting BiSb alloy tunnel junctions. A piece of $0.1 \times 0.2 \times 0.05$ cm³ of 1- Ω -cm As-doped Ge, kept at a distance of about 1 mm from the tunnel junction with an area of $\sim 10^{-4}$ cm², served as a photoconducting detector with an applied field of 15 V/cm in bulk.⁸ The tunnel junction together with the photodetector is immersed in pumped liquid helium. Relatively low-resistance tunnel junctions were selected so that high currents could be used, as shown in Fig. 3. Reproducible sudden polarizations to a slightly low-conductivity state at +0.25 V and to a slightly high-conductivity state at -0.27 V are noted.⁹ Both stable states may be explained on the basis of the charging and discharging of trap states on the surface or inside the thin insulating layer by the applied field. It is interesting that the observed photodetector current, a fraction of a nanoampere,

is always associated with the low-conductivity state as shown with heavy lines as a function of applied voltage, whereas no light emitted in the high-conductivity state as indicated by the dashed I - V curve in Fig. 3. Although we have not measured the photon spectrum yet, it must be $0.2 > h\nu > 0.02$ eV. In view of the nature of the BiSb-insulator-metal system illustrated in Fig. 2, one can conceive a few recombination processes, which might be accompanied by the photon emission.

Two conductance curves in Fig. 1(c) show the polarization effect in detail. Suppose initially it is the upper curve of the high-conductivity state. Then, it changes to the lower curve of the low-conductivity state, when polarized by applying +0.4-0.5 V. This state is stable unless one applies -0.4-0.5 V, at which it returns to the high-conductivity state. Two curves in Fig. 1(a) are also another example of this effect. Although one can obtain a continuous distribution of conductivity states, dependent upon the polarizing of the junction, the assigned values of band edges are virtually unchanged as seen in the figures.

The authors wish to thank D. F. O'Kane for carefully grown BiSb single-crystal alloys, S. H. Koenig and N. Wiser for many helpful suggestions, L. Alexander and J. Cummings for assistance in performing the experiments.

¹L. Esaki and P. J. Stiles, Phys. Rev. Letters **14**, 902 (1965).

²P. V. Gray, Phys. Rev. **140**, A179 (1965). We believe he made a rather serious mistake in the integration of tunneling current, Eq. (12), in his paper, as correctly pointed out by N. Wiser and, therefore, his Figs. 3 and 4 are also incorrect.

³A. L. Jain, Phys. Rev. **114**, 1518 (1959).

⁴D. M. Brown and S. J. Silverman, Phys. Rev. **136**, A290 (1964).

⁵S. Mase, J. Phys. Soc. Japan **13**, 434 (1958); **14**, 584 (1959).

⁶M. H. Cohen, L. M. Falicov, and S. Golin, IBM J. Res. Develop. **8**, 215 (1964).

⁷L. C. Hebel and G. E. Smith, Phys. Letters **10**, 273 (1964).

⁸S. H. Koenig and R. D. Brown, III, Phys. Rev. Letters **4**, 170 (1960).

⁹W. R. Hiatt and T. W. Hickmott, Appl. Phys. Letters **6**, 106 (1965).

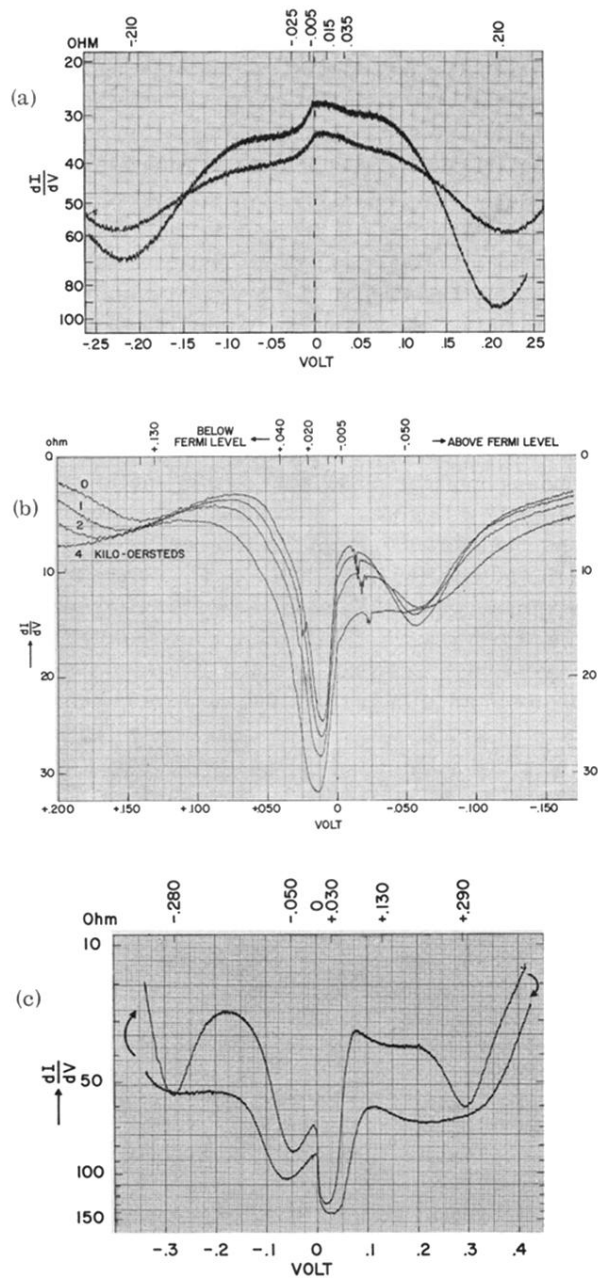


FIG. 1. Conductance versus voltage plots at 2°K. (a) 3.6% alloy tunnel junction; (b) 12.0% alloy tunnel junction, at magnetic fields parallel to the trigonal axis, 0, 1, 2, and 4 kOe; (c) 13.5% alloy tunnel junction, showing a polarization effect, high- and low-conductivity states.